RSC Advances

ROYAL SOCIETY OF CHEMISTRY

www.rsc.org/advances

Controllable Microdroplet Splitting via Additional Lateral Flow and its Application in Rapid Synthesis of Multi-scale Microspheres

Bingpu Zhou[1], Cong Wang[1], Xiao Xiao[2], Yu Sanna Hui[1], Yulin Cao[2], Weijia Wen[1,2*]

[1]Nano Science and Technology Program, The Hong Kong University of Science and Technology, Clear Water Bay, Kowloon, Hong Kong

[2]Department of Physics and KAUST-HKUST Micro/Nanofluidic Joint Laboratory, The Hong Kong University of Science and Technology, Clear Water Bay, Kowloon, Hong Kong

[*]To whom correspondence should be addressed: E-mail: phwen@ust.hk. Tel: +852-23587979; fax: +852-23581652.

Abstract

In this paper, we demonstrated that controllable microdroplet splitting could be obtained via additional lateral flow with simplicity and high controllability. The volume ratio of the two splitting products can be flexibly regulated by adjusting the flow rate ratio between the main and additional lateral flows. The splitting phenomena under different main flow rates were investigated. A volume ratio up to 200:1 of the two daughter droplets under a relatively higher main flow rate was experimentally achieved based on our approach. Under this case, we have successfully achieved uniform daughter droplets with smallest diameter of ~19.5±1.6 μm. With such design, we have synthesized uniform PEGDA hydrogel microspheres with diameters ranging from ~30 μm to over hundred of micrometers simultaneously.

Keywords: Droplet-based Microfluidics (DBMF); Controllable microdroplet splitting; Microgel synthesis; PEGDA (poly(ethylene glycol) diacrylate).

Introduction

Since its advent two decades ago, droplet-based microfluidics (DBMF) has attracted substantial interest owing to its several superiorities including smaller volume, faster reaction rate, and less cross-contamination[1-3]. To date, DBMF has been successfully applied in a broad range of research areas from bio-chemical analysis to electronic microsystems[4-7]. The rapid growth of these interdisciplinary fields demands for further advancements in droplet manipulations, design optimizations and process flow developments. Nowadays, various kinds of operations have been extensively studied in order to provide precise control of microdroplets in terms of droplet dimension, trajectory and concentration[8-13].

Droplet splitting is one of the most important operations in DBMF, in which droplets are fragmented into desired sizes for increasing droplet production efficiency, enhancing the capacity of up-scaling, and possibilities of parallel experiments[14-16]. The theoretical and experimental studies on these subjects have been widely investigated and reported in various literatures[17-19]. Passive splitting is generally based on geometry-mediated fission mechanism. It has been demonstrated that droplet splitting can be obtained steadily at precise locations such as 3D crossing microstructure[20], T-shaped junction[21], branching channels[22], and artificial obstacle inside the channel[23]. Although these approaches do not rely on peripheral controls, the volume of the split droplet is confined by the fixed geometry with limited amount of control dynamics and flexibility. In contrast, active droplet splitting can be achieved by external sources such as electricity or heat. For example, electric field can be used to split polarized uncharged droplets at the bifurcating junction[24]. Localized heating by laser can be utilized as a thermocapillary valve which dynamically controls the volume ratio of the two daughter droplets[25]. Other active droplet splitting methods including EWOD (Electro-wetting on dielectric), integrated microheater patterns and pneumatic actuators have been successfully achieved[26-28]. However, adopting peripheral control requires additional components for control circuitry, and may increase the complexity of the overall design. Additionally, the use of electrical and thermal power may discourage the applications in bio/chemical objects owing to the sustainability of electrical or thermal damage.

In this work, we proposed and demonstrated that controllable droplet splitting could be achieved

with tunable lateral flow at the location of a bifurcation without any changing on the microchannel geometry or requirement of external actuators. By simply adjusting the flow rate ratio between the main and the lateral flow, the volume ratio of daughter droplets can be dynamically regulated and achieved up to a high ratio of 200:1. Such technique can be well applied for on-chip controllable droplet splitting with tunable and precisely desired ratios. Based on the proposed technique, uniform PEGDA hydrogel microspheres with multi-sizes ranging from ~30 μm (diameter) to over hundred of micrometers were successfully synthesized.

Methods

Design principle

Fig. 1a illustrates the 3D configuration of our microfluidic chip design. The width of the microchannel is designed of 200 μm. A flow-focusing region is utilized to generate uniform mother droplets for further splitting. Inlet 1 (Q_1) is for continuous phase injection and Inlet 2 (Q_2) is for the dispersed phase. The serpentine channel components are designed in order to damp the changes in pressure in the droplet generation junction to ensure stable and uniform mother droplet formation. The generated mother droplet then runs along the microfluidic channel and approaches the bifurcation for splitting. The bifurcation is composed of a main fluidic channel and another fluidic channel branched off at 30 degree angle as indicated in the inset. Inlet 3 (Q_3) provides additional lateral continuous flow which deflects the mother droplet towards the vicinity of the bifurcation. All three liquid inlets are controlled separately via external syringe pumps. Ports numbered 4 and 5 are outlets for fluid draining.

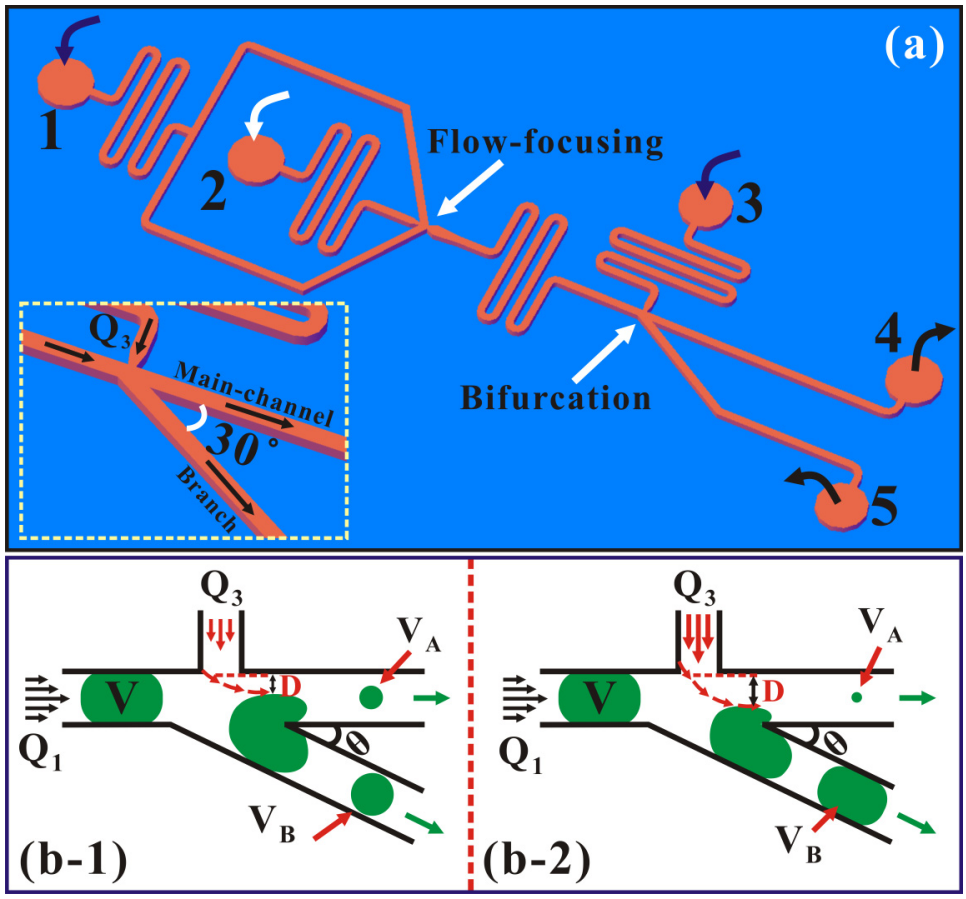

Fig.1 (a) 3D configuration of microfluidic chip for controllable droplet splitting. The inset gives an enlarged view of the bifurcation; (b) Illustration of controllable splitting with two different values of the lateral flow rate (left: smaller Q_3; right: larger Q_3).

Traditionally for splitting mechanism based on artificial bifurcations, the volume ratio of the two daughter droplets will be mainly controlled via the downstream flow resistance of the two branches according to Hagen-Poiseuille law. On this occasion, the volume ratio of the two divided daughter droplets will lack of flexibility without modification on the geometry of the microchannel. In this work, we combine additional lateral flow with the bifurcation junction to obtain controllable microdroplet splitting as depicted in Fig. 1b. When approaching the bifurcation, the mother droplet is pushed by the lateral flow to the vicinity of the bifurcation junction. The vertical displacement of the mother droplet, D (Fig. 1b), is mainly determined by the ratio of Q_3 and Q_1, and a higher Q_3/Q_1 results in a larger D. The value of D, hence, determines the relative position of the droplet to the bifurcation, and has an important impact on the final splitting ratio between two daughter products. With a smaller Q_3 (Fig. 1b-1), D is relatively small which leads to a relatively smaller portion of the mother droplet into the

branch. With a larger Q_3 (Fig. 1b-2), D becomes relatively larger such that a larger portion of the mother is split into the branch. On this occasion, we can find out that with a larger and larger Q_3 (constant Q_1), the volume of daughter droplets into the branch will increase which finally diminishes the value of V_A/V_B.

In principle, Q_3/Q_1 can be used to regulate the splitting ratio of the daughter droplet's volume ratio (V_A/V_B). Since Q_3 is regulated separately via the syringe pump, the splitting ratio can be adjusted simply by tuning the exact lateral flow without any adjustment on the mother droplets or the device geometry. Such an approach can help one to restructure the volumes of droplet products at will without any requirement of external electrical, mechanical or thermal actuations.

Fabrication, materials and operation

Fabrication of the microfluidic chip adopted standard soft lithographic protocol to obtain microchannel structures in polydimethylsiloxane (PDMS). To prepare reusable mold for the microchannel, SU8-3025 (MicroChem Corp., USA) with thickness of ~40 μm was patterned on a clean glass substrate. PDMS gel (Sylgard 184 silicone elastomer kit, Dow Corning Corporation, USA) was then prepared by mixing the base with curing agent at a weight ratio of 10:1 before applying it to the glass mold. After solidification, the PDMS slab was peeled off from the mold, with the channel structure successfully transferred. The PDMS casted with the microchannel patterns was bonded to another flat PDMS slab using oxygen plasma surface treatment for ~2 mins. Finally, a hard baking process (at 100°C, 10 min) concluded the entire microfluidic chip fabrication procedure.

DI-water and sunflower oil were used as the dispersed and continuous phase respectively in demonstration of controllable microdroplet splitting. Oil Red O (Sigma-Aldrich Co., USA) and Oil Blue N (Sigma-Aldrich Co., USA) were dissolved into sunflower oil for purpose of better color contrast. For application illustration of microsphere synthesis, a hydrogel material, PEGDA (poly(ethylene glycol) diacrylate, Sigma-Aldrich) was employed as the dispersed phase by dissolving it in DI-water with a volume ratio of 1:4. Photo-initiator (2-Hydroxy-4'-(2-hydroxyethoxy)-2-methylpropiophenone 98%, International Laboratory, USA) was uniformly added to the hydrogel solution with a mass concentration of 1mg/ml. Mineral oil (Sigma), mixed with Span-80 (Sigma-Aldrich) by a weight ratio of 2%, was used as the carrier fluid. Here

Span-80 served as the surfactant to prevent PEGDA droplet coalescences inside the microchannel.

Liquid injections in this work were precisely performed by using 500 µL glass syringes (#1750, Hamilton, USA) and syringe pumps (PHD2000, Harvard Apparatus, Holliston, USA). Experimental videos were captured in real-time under the optical microscope (SZX16 with DP71 CCD, Olympus Corporation, Tokyo, Japan). The detailed information of the obtained daughter droplets were analyzed using ImageJ Software (Version 1.47, National Institutes of Health, USA). UV-light source (ELC-450 UV light spot-cure system) with output of 5.0 W/cm^2 at 365 nm was utilized to quickly obtain polymerized microspheres in the application demonstration section.

Results and Discussion

Controllable splitting with tunable lateral flow rate (Q_3)

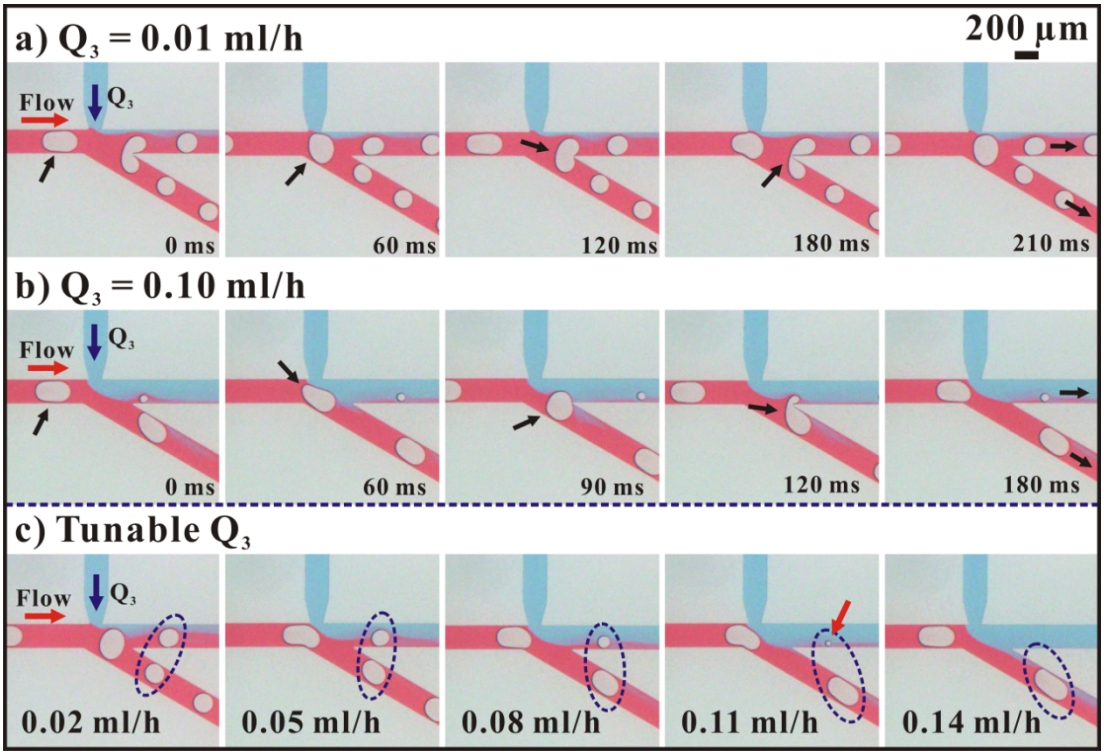

Fig. 2 (a), (b) A Series of still photos captured in sequence to illustrate droplet splitting process under two typical values of Q_3; (c) Different splitting results based on the tunable values of Q_3. The paired daughter droplets were indicated by blue ellipses. The scale bar is valid for all of the included photos.

Firstly, we investigated the microdroplet splitting process under different ratios between the main and lateral flow rates (Q_3/Q_1). Here, Q_1 and Q_2 were kept constantly at 0.06 ml/h and 0.02 ml/h, respectively. During the process, we gradually increased Q_3 from 0.01ml/h to 0.14 ml/h. Fig. 2a and b show a series of still photos captured in sequence for illustrating droplet splitting process under two typical values of Q_3 (0.01ml/h and 0.10 ml/h). As shown in Fig. 2a, with a relatively low Q_3 (0.01 ml/h), the deflection of mother droplet from the vertical locations was fairly small and could be ignored. In this case, the portion of the mother droplet navigated into the branch would mainly depend on the downstream flow resistances. As in our design, the two downstream flow resistances were almost the same such that the volume ratio of the two daughter products remained as about 1.17±0.02 in this situation. While with increased Q_3 to 0.10 ml/h (Fig. 2b), it could be found that the mother droplet was deflected dramatically to the bifurcation. As a consequence, a relative large portion of the mother droplet was passively split into the branch, resulting in a small value of V_A/V_B to be 0.09±0.01. From the results mentioned above, we could find that with a constant main flow rate, the displacement of the mother droplet would be mainly regulated via Q_3, which finally helped to tune V_A/V_B in a simple manner. Fig. 2c describes different splitting outcomes based on the diverse lateral flows ranging from 0.02 ml/h to 0.14 ml/h. It could be found that a larger Q_3 led to a larger portion of the mother droplet into the branch and thus a smaller V_A/V_B. The smallest daughter droplets (indicated via the red arrow) with diameter of around 47.0±0.4 μm were obtained in the main channel when Q_3 was set at 0.11 ml/h, namely Q_3/Q_1 was almost 1.83. With further increased Q_3 (0.14 ml/h), the mother droplet was completely deflected into the branch without successful splitting as given in the final photo of Fig. 3c. The real-time records of such a controllable microdroplet splitting process could be found in the supplementary materials. The above results demonstrated that controllable splitting could be simply achieved via tuning additional lateral flow in the downstream of the microfluidic channel, without any demand to modify the geometry of the microchannel or the size of the mother droplets.

Controllable splitting under different main flow rates

In this subsection, the splitting process under different main flow rates (Q_1) was investigated. Fig. 3a shows the relationship between the flow rate ratio (Q_3/Q_1) and the daughter droplet volume ratio (V_A/V_B) for four different Q_1. The size of the mother droplet for each case was kept the same by

precisely setting value of Q_1 and Q_2. For each Q_1, we gradually changed Q_3 to obtain tunable splitting outcomes while keeping Q_1 and Q_2 as constants. From the four graphs, it could be obviously found that tunable splitting volume ratios could be acquired based on changing the lateral flow rates for all main flow rates. With increased Q_3 (thus larger Q_3/Q_1), the obtained V_A/V_B gradually decreased since a larger portion of the mother droplet was deflected into the branch.

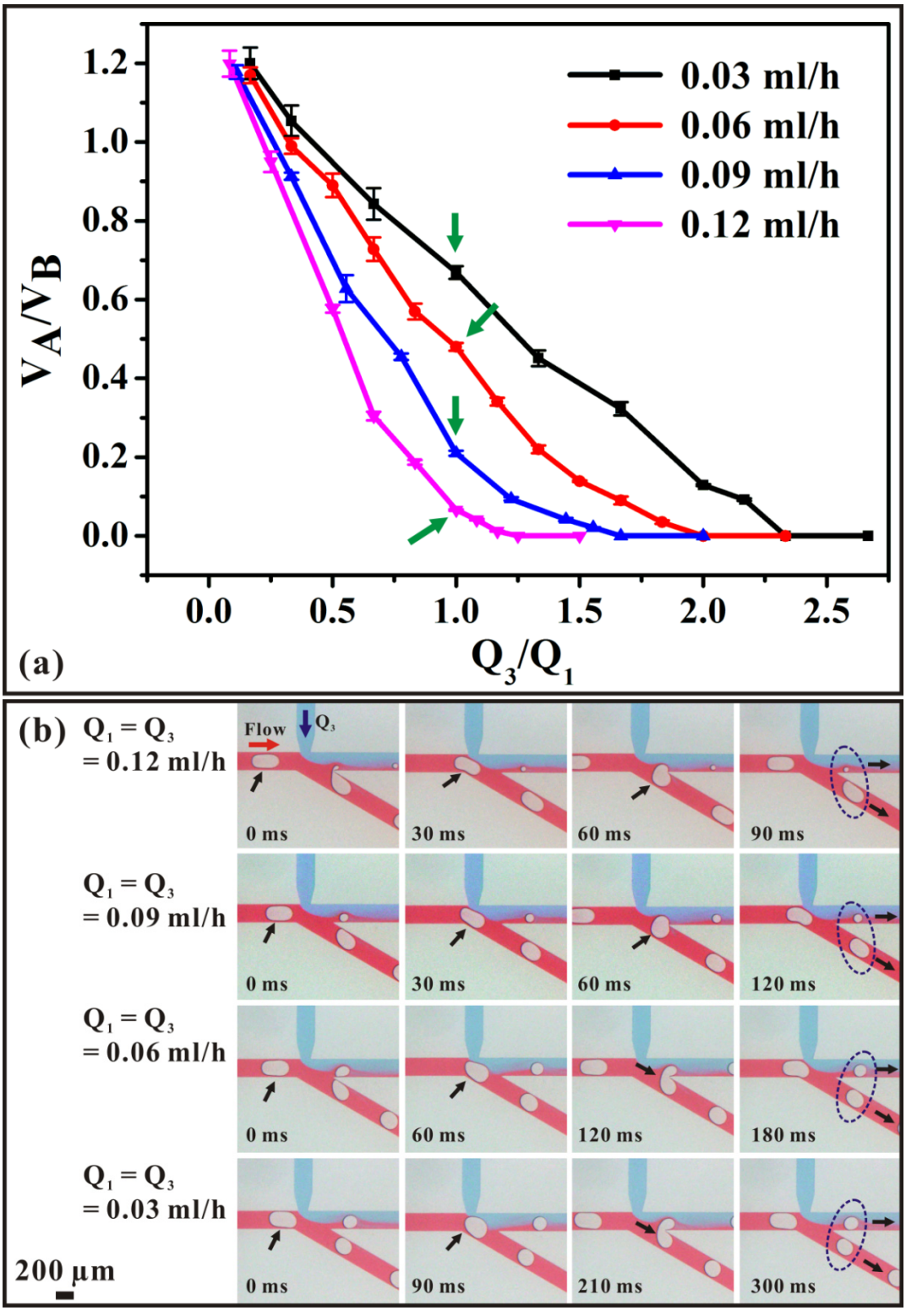

Fig. 3 (a) Relationship between V_A/V_B and Q_3/Q_1 under different values of Q_1;

(b) Splitting results of different main flow rates with the same value of Q_3/Q_1. The paired daughter droplets have been marked with blue ellipses in the final frame of each case.

In addition, from the curves we could observe that for a specific Q_3/Q_1, the value of V_A/V_B was smaller with a larger Q_1. Take Q_3/Q_1 of 1.0 as an example (indicated via the green arrows in Fig. 3a), when Q_1 was 0.03 ml/h, the volume ratio of two daughter droplets was 0.669±0.016. When Q_1 was changed to 0.06 ml/h, 0.09 ml/h and 0/12 ml/h, V_A/V_B gradually decreased to 0.480±0.010, 0.210±0.006 and 0.066±0.002. The splitting processes for all four cases were illustrated in Fig. 3b. A proper explanation to the phenomena could be that with the same Q_3/Q_1, the splitting volume ratio would be mainly defined by the residence time of the mother droplet at the location of the bifurcation. When the mother droplet approached the bifurcation, it was deflected from the vertical position via the lateral flow as aforementioned. During this process, the shape of the mother droplet deformed (as shown in Fig. 3b) to match the corresponding flow path in the downstream. With a higher main flow rate, thus the higher velocity, the mother droplet was deflected into the branch and divided at the bifurcation before complete deformation. Under this circumstance, a larger portion of the mother droplet was deflected and split into the branch resulting in a smaller volume ratio of the two daughter products. On the contrary, a smaller main flow rate rendered a more sufficient residence time for the mother droplet to deform at the bifurcation such that V_A/V_B would be larger even with the same Q_3/Q_1. From this perspective, we could conclude that the main flow rate, thus the velocity of the mother droplet, plays an important role in defining the final splitting volume ratios.

Obtained smallest daughter droplets under different main flow rates

Here we will mainly focus on the dimension of the smallest daughter droplets that we have obtained under different main flow rates (Q_1). Four cases of Q_1 were investigated here, namely 0.03 ml/h, 0.06 ml/h, 0.09 ml/h and 0.12 ml/h as above. Fig. 4 shows the smallest daughter droplets which could be stably and uniformly obtained under different Q_1. For Q_1 of 0.03 ml/h, the smallest daughter droplet with diameter of ~81.7±0.7 μm was obtained when Q_3 was set of 0.065 ml/h. When Q_1 was increased to 0.06 ml/h and 0.09 ml/h, the diameters of the smallest daughter droplets obtained in the main channel diminished to ~47.0±0.4 μm and ~32.5±0.8 μm (enlarged view in the inset), respectively. With the highest investigated Q_1 (0.12 ml/h), it was found that the smallest daughter droplet with diameter of ~19.5±1.6 μm (enlarged view in the inset) could be achieved when Q_3 increased to 0.14 ml/h. It was found that the dimension variation of daughter droplets was relatively larger when diameter was

decreased to ~19.5 μm. This may be caused by the instability of flows in the downstream in such a condition. For this case, it was calculated that the volume ratio of the two daughter droplets reached an extremely high value of around 0.005±0.001 (V_B: $V_A \approx 200$: 1). Here the daughter droplet in the main channel was deemed as a sphere because the diameter was smaller than the height of the microchannel (~40 μm). For all cases of Q_1, the mother droplet was deflected completely into the branch without successful splitting when we further increased the lateral flow rates.

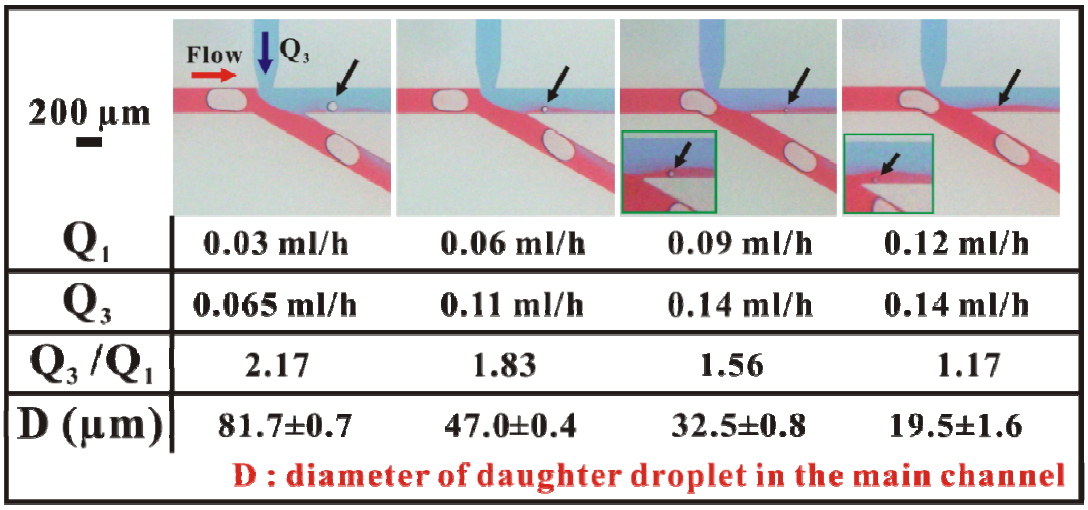

Q_1	0.03 ml/h	0.06 ml/h	0.09 ml/h	0.12 ml/h
Q_3	0.065 ml/h	0.11 ml/h	0.14 ml/h	0.14 ml/h
Q_3/Q_1	2.17	1.83	1.56	1.17
D (μm)	81.7±0.7	47.0±0.4	32.5±0.8	19.5±1.6

D : diameter of daughter droplet in the main channel

Fig. 4 Obtained smallest daughter droplets under different Q_1. For Q_1 of 0.09 ml/h and 0.12 ml/h, the daughter droplets in the main channel were enlarged in the insets due to the relatively small sizes.

This phenomenon revealed that smaller daughter products could be divided out from the mother droplet into the main channel with a relatively higher main flow rate (higher velocity of the mother droplet). Actually, we have attempted to realize even smaller daughter droplets for case of smaller Q_1 (e.g. Q_1 of 0.03 ml/h). However, we found that even with a slightly enhanced Q_3, such as 0.068 ml/h or 0.070 ml/h, the mother droplet was entirely pushed into the branch without splitting at all. To address this critical issue, the capillary number (*Ca*) was adopted to find out the relationship between the volume of the smallest daughter droplet and the main flow rate. *Ca* is given by equation (1)

$$Ca = \frac{\eta\mu}{\gamma} \qquad (1)$$

where γ is the interfacial tension between the continuous and dispersed phase, η and μ are the dynamic viscosity and velocity of the continuous phase, respectively. As in our microfluidic system, η and γ were kept constant such that *Ca* would be mainly affected by μ. With a higher μ, *Ca* would

accordingly increase resulting in a decrease of the size of the obtained daughter droplet. From this perspective, we could conclude that a higher velocity of the mother droplet would lead to the production of smaller daughter products based on our splitting approach.

Application: Controllable splitting for multi-scale microsphere synthesis

Microfluidics has been proved to be a novel platform for the production of monodisperse microparticles with specific structures or properties during the past decade[29-33]. In particular, synthesis of microgels via microfluidic techniques has evolved rapidly due to their low toxicity and biocompatibility for a broad range of applications[30, 34-36]. Until now, Microgel particles generated from microfluidic chip have been widely applied in many areas including cell encapsulation, drug delivery, and anisotropic magnetic response materials[37-39]. Although such microfluidic approaches provide useful venue for production of functional microgel particles, there still remains intrinsic obstacles. Firstly, the generation rate cannot be greatly improved based on single droplet source. Even if mass production of droplets can be somehow relieved by parallelization of micro-junctions, it may also bring in a more complex channel design for the size sorting of microgel particles. Secondly, it is difficult to obtain a wide dimensional range of microgel particles simultaneously by simply changing the relative micro-flow rate owing to the limitation raised by the fixed channel geometry. Although synthesis of microgel spheres with different sizes has been widely studied, it is still a challenge to obtain microspheres with relatively wide scale-range simultaneously via a single device. With the controllable splitting technique presented earlier, here we demonstrated that PEGDA microgel spheres with dimension ranging from ~30 μm to over hundred of micrometers could be achieved in situ. This technique does not rely on external power such as electricity, pressure or heat for regulation of the particle sizes. Microgel spheres with diverse desired sizes could be obtained and sorted at two different collection outlets by simply tuning the lateral flow rates.

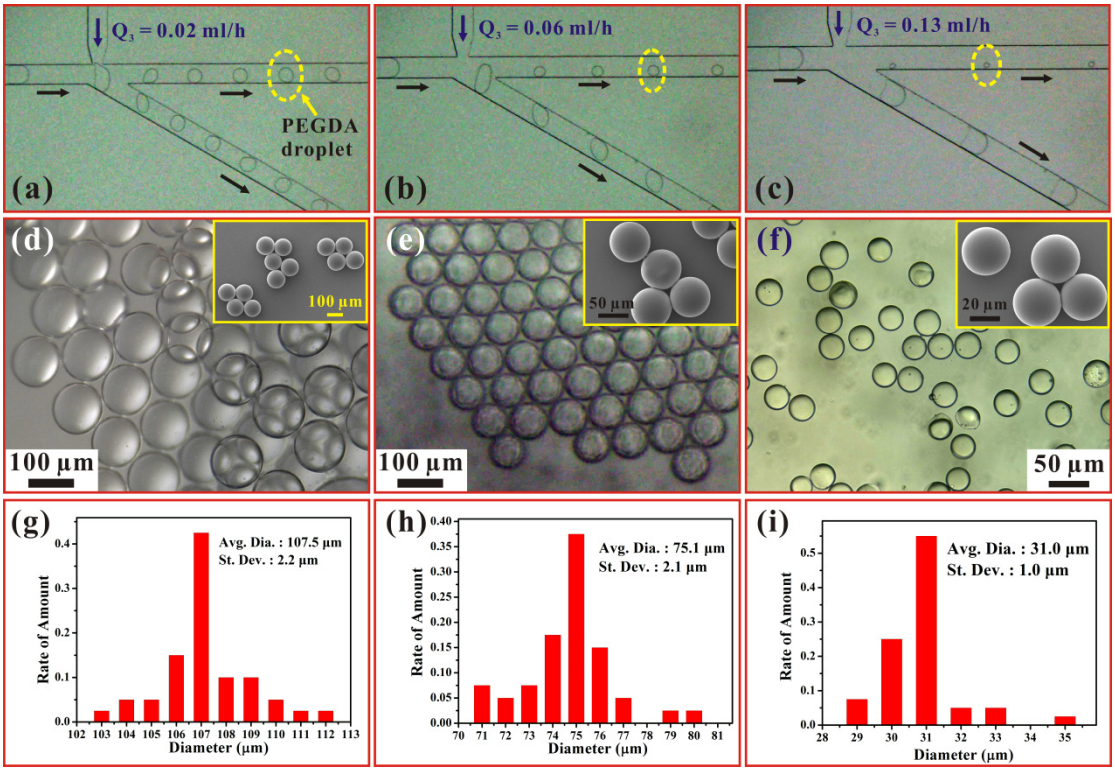

Fig. 5 (a)-(c) Optical images that illustrate synthesis of microgel particles with different lateral flows (tunable splitting ratios); (d)-(f) Optical images of PEGDA particles successfully synthesized. The insets are SEM images indicating the close-up of the particle morphology; (g)-(i) Size distribution of the microgel particles corresponding to images (d)-(f).

The flow direction of droplet arrays is indicated by the black arrow in Fig. 5(a). Fig. 5 (a)-(c) give the controllable splitting results of PEGDA emulsions based on tuning the lateral flow. Here Q_1 and Q_2 were kept at 0.12 ml/h and 0.04 ml/h, respectively. To demonstrate, the flow rates of the lateral flow for three conditions were set as 0.02 ml/h, 0.06 ml/h and 0.13 ml/h as indicated. It should be noticed here that the relationship between the volume ratios of two daughter droplets and the flow rate ratios may be slightly different from the aforementioned demonstration due to the change of interfacial tension (γ). However, it could also be clearly found that the splitting phenomenon was comparable to the experimental results of droplet splitting described previously. The volume of the daughter droplets inside the main channel gradually decreased with increase of the lateral flow (Q_3). The products from the outlets were drained via respective Tygon tubing and exposed to ultraviolet irradiation for ~5 mins. The irradiation resulted in polymerization of microgel particles and finally solidified into spheres. These microgel spheres were collected via a microtube, washed with ethanol/deionized water and

finally segregated from the oil by the centrifuge.

Optical images of synthesized PEGDA microgel spheres are shown in Fig. 5(d)-(f). The insets are the SEM images of the uniform microgel spheres synthesized which clearly describe the morphology of the obtained microparticles. Fig. 5(g)-(i) show the size distributions of synthesized microspheres. From these graphs, one can observe that the average size of each group of spheres are about 30 μm, 75.1 μm and 107.5 μm respectively, with a small standard deviation of 1.0 μm, 2.1 μm and 2.2 μm. In this report, we present the results of successful synthesis of spheres that are relatively small in size. For larger microspheres (several hundreds of micrometers), it is obviously much easier to synthesize by increasing the dimension of the mother droplet. Similar splitting results with larger mother droplets have also been widely investigated in many reports. The experimental results have indicated that uniform microspheres can be synthesized using the dynamic splitting technique explained above. The synthesized microspheres have a diameter ranging from about 30 μm to over hundred of micrometers. For microspheres smaller than 30 μm, we are in the process of exploring other approaches such as reducing the height of the channel, the size of the mother droplet, and tuning the branching angle at the bifurcation. Such approach can realize a higher degree of controllability and production rate for micro-object fabrications.

Conclusion

We have proposed, fabricated and successfully demonstrated the controllable droplet splitting technique via an additional lateral flow at the bifurcation. Splitting ratio up to 200:1 has been achieved by precisely tuning the ratio of the lateral and the main channel flow rate. With a higher flow rate, daughter droplet with small diameter of ~20 μm has been successfully realized. Based on this design, we have also synthesized uniform PEGDA microgel spheres with multi-sizes ranging from ~30 μm to over hundred of micrometers simultaneously which is considered difficult to realize by conventional passive or active splitting methods. The proposed microsphere synthesis approach exhibits high-throughputs with on-demand size selection at desired channel outlets. The dimension of microspheres can easily be regulated by tuning the lateral flow rates. We believe that this novel technique for controllable splitting could be widely used not only in microfluidic area but also in other technical bio/chemical research fields.

Acknowledgements

The authors would like to acknowledge the support by Hong Kong RGC grant HKUST 605411 and NSFC/RGC joint grant N_HKUST601/11. The work was also partially supported by the Nanoscience and Nanotechnology Program at HKUST.

References

[1] J. Atencia, and D. J. Beebe, Nature, 437, (2009) 648-655.

[2] G. M. Whitesides, Nature, 442, (2006) 368-373.

[3] D. T. Chiu, R. M. Lorenz, and G. D. M. Jeffries, Anal. Chem., 81, (2009) 5111-5118.

[4] M. Prakash, and N. Gershenfeld, Science, 315, (2007) 832-835.

[5] S. Duraiswamy, and S. A. Khan, Small, 5, (2009) 2828-2834.

[6] A. B. Theberge, F. Courtois, Y. Schaerli, M. Fischlechner, C. Abell, F. Hollfelder, and W. T. S. Huck, Angew. Chem. Int. Ed., 49, (2010) 5846-5868.

[7] G. T. Vladisavljevic, I. Kobayashi, and M. Nakajima, Microfluid Nanofluid, 13, (2012) 151-178.

[8] B. Zheng, J. D. Tice, and R. F. Ismagilov, Anal. Chem., 76, (2004) 4977-4982.

[9] Y. C. Tan, Y. L. Ho, and A. P. Lee, Microfluid Nanofluid, 4, (2008) 343-348.

[10] Z. Z. Che, N. T. Nguyen, and T. N. Wong, Appl. Phys. Lett., 98, (2011) 054102.

[11] B. Ahn, K. Lee, H. Lee, R. Panchapakesan, L. Xu, J. Xu, and K. W. Oh, Lab Chip, 11, (2011) 3915-3918.

[12] J. Xu, B. Ahn, H. Lee, L. Xu, K. Lee, R. Panchapakesan, and K. W. Oh, Lab Chip, 12, (2012) 725-730.

[13] Z. Cao, F. Chen, N. Bao, H. He, P. Xu, S. Jana, S. Jung, H. Lian, and C. Lu, Lab Chip, 13, (2013) 171-178.

[14] S. Y. The, R. Lin, L. H. Hung, and A. P. Lee, Lab Chip, 8, (2008) 198-220.

[15] A. R. Abate, and D. A. Weitz, Lab Chip, 11, (2011) 1911-1915.

[16] R. Seemann, M. Brinkmann, T. Pfohl, and S. Herminghaus, Rep. Prog. Phys., 75, (2012) 01660.

[17] D. R. Link, S. L. Anna, D. A. Weitz, and H. A. Stone, Phys. Rev. Lett., 92, (2004) 054503.

[18] V. Cristini, and Y. C. Tan, Lab Chip, 4, (2004) 257-264.

[19] A. Carlson, M. D. Quang, and G. Amberg, Int. J. Multiphase Flow, 36, (2010) 397-405.

[20] Y. T. Chen, W. C. Chang, W. F. Fang, S. C. Ting, D. J. Yao, and J. T. Yang, Microfluid Nanofluid, 13, (2012) 239-247.

[21] Y. C. Tan, J. S. Fisher, A. I. Lee, V. Cristini, and A. P. Lee, Lab Chip, 4, (2004) 292-298.

[22] T. Moritani, M. Yamada, and M. Seki, Microfluid Nanofluid, 11, (2011) 601-610.

[23] S. Protiere, M. Z. Bazant, D. A. Weitz, and H. A. Stone, EPL, 92, (2010) 54002.

[24] D. R. Link, E. G. Mongrain, A. Duri, F. Sarrazin, Z. Cheng, G. Cristobal, M. Marquez, and D. A. Weitz, Angew. Chem. Int. Ed., 45, (2006) 2556-2560.

[25] C. N. Baroud, J. P. Delville, F. Gallaire, and R. Wunenburger, Phys. Rev. E, 75, (2007) 046302.

[26] S. K. Cho, H. Moon, and C. J. Kim, J. Microelectromech. Syst., 12, (2003) 70-80.

[27] Y. F. Yap, S. H. Tan, N. T. Nguyen, S. M. S. Murshed, T. N. Wong, and L. Yobas, J. Phys. D, 42, (2009) 065503.

[28] J. H. Choi, S. K. Lee, J. M. Lim, S. M. Yang, and G. R. Yi, Lab Chip, 10, (2010) 456-461.

[29] S. Xu, Z. Nie, M. Seo, P. Lewis, E. Kumacheva, H. A. Stone, P. Garstecki, D. B. Weibel, I. Gitlin, and G. M. Whitesides, Angew. Chem. Int. Ed., 44, (2005) 724-728.

[30] H. Zhang, E. Tumarkin, R. M. A. Sullan, G. C. Walker, and E. Kumacheva, Macromol. Rapid Commun., 28, (2007) 527-538.

[31] D. Dendukuri, and P. S. Doyle, Adv. Mater., 21, (2009) 4071-4082.

[32] S. Lone, S. H. Kim, S. W. Nam, S. Park, J. Joo, and I. W. Cheong, Chem. Commun., 47, (2011) 2634-2636.

[33] K. Jiang, P. C. Thomas, S. P. Forry, D. L. DeVoe, and S. R. Raghavan, Soft Matter, 8, (2012) 923-926.

[34] J. I. Park, A. Saffari, S. Kumar, A. Gunther, and E. Kumacheva, Annu. Rev. Matter. Res., 40, (2010) 415-443.

[35] J. Wan, Polymers, 4, (2012) 1084-1108.

[36] Y. Hu, Q. Wang, J. Wang, J. Zhu, H. Wang, and Y. Yang, Biomicrofluidics, 6, (2012) 026502.

[37] L. K. Fiddes, E. W. K. Young, E. Kumacheva, and A. R. Wheeler, Lab Chip, 7, (2007) 863-867.

[38] D. K. Hwang, D. Dendukuri, and P. S. Doyle, Lab Chip, 8, (2008) 1640-1647.

[39] P. Panda, S. Ali, E. Lo, B. G. Chung, T. A. Hatton, A. Khademhosseini, and P. S. Doyle, Lab Chip, 8, (2008) 1056-1061.